# Graphane Nanotubes

**Xiao-Dong Wen,[†,§,*] Tao Yang,[†] Roald Hoffmann,[†,*] N. W. Ashcroft,[‡] Richard L. Martin,[§] Sven P. Rudin,[§] and Jian-Xin Zhu[§]**

[†]Department of Chemistry and Chemical Biology, Baker Laboratory, Cornell University, Ithaca, New York 14853-1301, United States, [‡]Laboratory of Atomic and Solid State Physics and Cornell Centre for Materials Research, Clark Hall, Cornell University, Ithaca, New York 14853-2501, United States, and [§]Theoretical Division, Los Alamos National Laboratory, Los Alamos, New Mexico 87545, United States

**ABSTRACT**

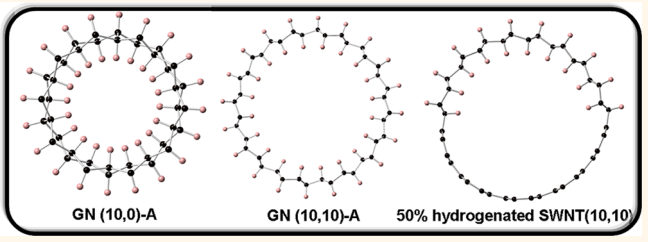


**In this work, one-dimensional graphane nanotubes (GN, stoichiometry CH), built from 2D single-sheet graphanes, are explored theoretically. Zigzag type GN(10,0) and armchair type GN(10,10) structures with varying surface termination were investigated in detail. GN(10,10)-A is found to be the most stable configuration among the GN structures considered. An annealing analysis indicates that graphane-A and GN(10,10)-A are likely to be stable at elevated temperature. A possible reaction path to GN(10,10)-A is suggested by the reaction of single-walled carbon nanotube (10,10) + $H_2$; the indications are that the GN(10,10)-A can be made at low temperature and high partial pressure of $H_2$ gas from the corresponding nanotube. The graphane nanotubes are predicted to be wide band gap insulators. A study of the effect of the diameter of GN structures shows, unexpectedly, that the gap increases on reducing the diameter of the graphane nanotubes. We also investigated several partially hydrogenated graphenes and single-walled carbon nanotubes (SWNT); the greater hydrogenation is, the more stable is the resulting structure. The band gap of graphene or SWNT can be tuned *via* hydrogenation.**

**KEYWORDS:** graphane sheets · graphane nanotubes · partially hydrogenated graphenes and nanotubes · band gap

Recent advances in the field of nanotechnology have led to the synthesis and characterization of an assortment of 1D and 2D (or quasi-1D and quasi-2D) nanostructures, such as tubes, wires, sheets, *etc.* The distinctive electronic properties of these fascinating materials are a consequence of their unique geometries. Low-dimensional, topologically diverse materials are potential building blocks for a wide range of nanoscale electronic, optoelectronic, magnetoelectronic, and sensing devices. Many techniques have been developed to grow such structures, not just for group 14,[1] but also for group III–V semiconductors, and metals.[2]

The two-dimensional graphane network (of stoichiometry CH) was first suggested by Sluiter and Kawazoe,[3] and by Sofo *et al.*,[4] with an approach to its synthesis made in 2009 by Elias *et al.*[5] using exposure of a single-layer graphene to a hydrogen plasma. Graphane is a wide band gap insulator, yet graphane–graphene mixed structures offer greater possibilities for the manipulation of the material's semiconducting properties.

In our previous work,[6] the four most stable two-dimensional (2D) single-sheet graphanes—two built on chair, two on boat cyclohexane motifs—were identified. The four isomeric two-dimensional sheets of stoichiometry CH, labeled A ("chair1"), B ("chair2"), C ("boat1"), and D ("boat2"), are shown in Figure 1. Interestingly, these isomers are more stable thermodynamically than even the archetypical aromatic benzene.[7] At $P$ = 1 atm the chair-boat differential, long known and understood in organic chemistry, governs the relative energy of the various graphane sheets. At higher pressures, for example, 300 GPa, lattices built from two sheet types that are not so stable at atmospheric pressure, chair2 and boat1, become enthalpically favored in our calculations.

Now, an interesting question arises which we answer in this paper: could one actually `roll up' the 2D graphane single sheets to form 1D graphane nanotubes? The analogy has proven profitable for the unsaturated all-carbon nets. Obviously dimensionality affects functionality; in a number of ways carbon nanotubes are different from graphene and graphite. Such graphane nanotubes (GN) would also be all-carbon nanotubes fully hydrogenated on the inside and outside of the carbon tube.

In this work, we have therefore explored some 1D GN structures built from the 2D graphane sheets shown above. The particular structures chosen for initial consideration are

* Address correspondence to rh34@cornell.edu, xwen@lanl.gov.

Received for review May 18, 2012 and accepted June 30, 2012.

**Published online June 30, 2012**
**10.1021/nn302204b**

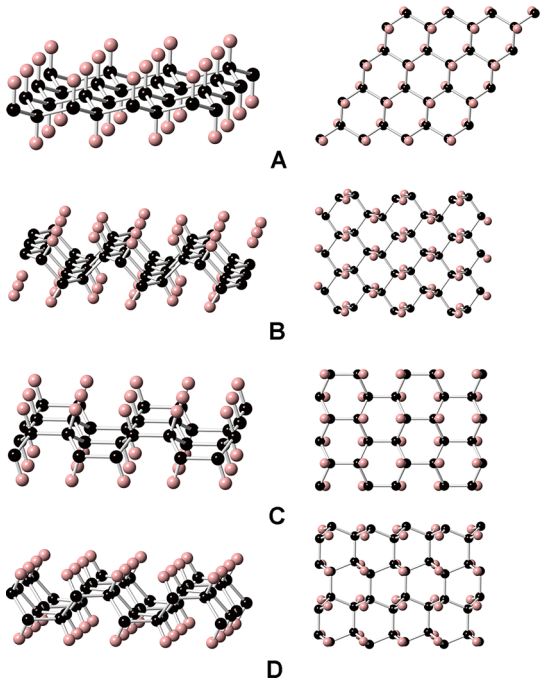


**Figure 1. Four isomeric single-sheet graphanes. Side views are at left, top views at right.**

the armchair (10,10) and zigzag (10,0) type GNs. Each graphane isomer (A, B, C, D above) then leads to two nanotubes. The relative stability of the nanotube can be measured by the enthalpy of the reaction ($C_x + {}^{x}/_{2}H_2 \rightarrow xCH$) for forming the GN, as a function of temperature and also of pressure in extended states. An *ab initio* annealing analysis, which heats a system to a specific temperature and then allows it to cool slowly, is performed. In addition, we explore some partially hydrogenated nanotubes.

We should make clear at the outset that we are not undertaking in this paper the immense task of finding the most stable partially or fully hydrogenated nanotubes. It is clear from fullerene studies[8−12] that if hydrogenation occurs, it will occur on both the inside and the outside of a fullerene, and that the most stable structure may not be fully hydrogenated. In this initial study we only build some in−out fully hydrogenated nanotubes based on stable graphane sheets, returning to the problem of optimal hydrogenation in future work.

## RESULTS AND DISCUSSIONS

**Structures and Energies of Hypothetical GNs.** Figure 2 shows front views and side views of four geometry-optimized zigzag GN (10,0) and four armchair GN (10,10) isomers. The nanotube types are labeled as A, B, C and D, by reference to the 2D graphane sheets used in their construction (see Figure 1). In Figure 3, we show the landscape of computed relative energies (per CH, relative to graphane-A) for these 2D graphane sheets and 1D GN structures, as well as the benzene

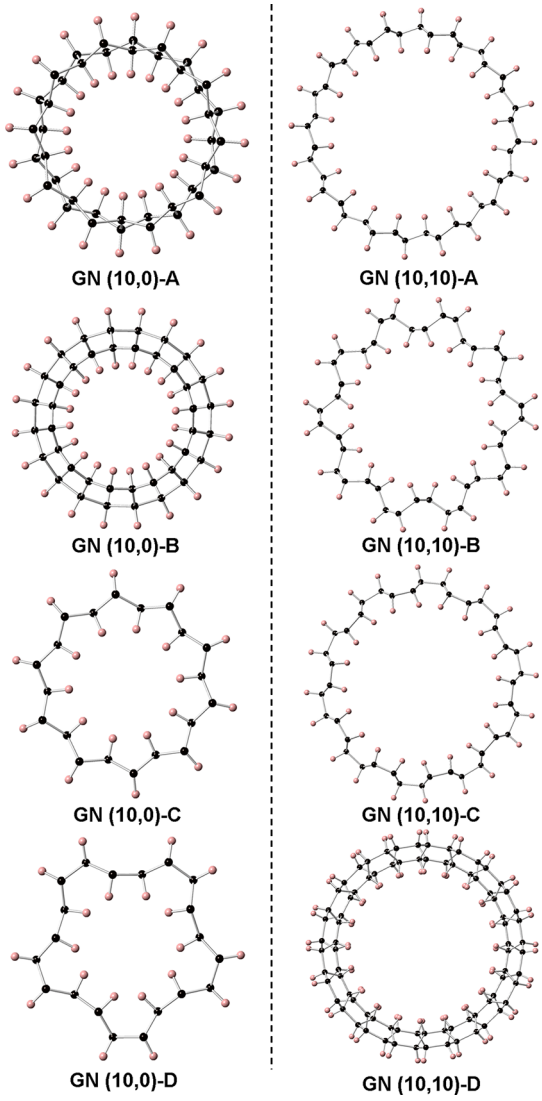


**Figure 2. Left: Four isomeric graphane nanotube (10,0) structures. Right: Four isomeric graphane nanotube (10,10) structures. For each type of GN, end-on views are shown (more views can be found in the Supporting Information).**

molecule. Zero point energies are not included in these calculations; they should be very similar in all the graphane structures considered here, as all of them have the same bonding patterns.

As one can see from Figure 3, 2D graphane-A is the most stable structure among all the isomers. Note the graphanes A−D are all more energetically stable than benzene, as discussed in our previous study.[6,7] Among the 1D GN structures, the GN (10,10)-A is thermodynamically the most favorable one, higher in energy than graphane-A and graphane-B, yet lower in energy than benzene molecule, graphane C and D. It is not surprising that the 1D GN(10,10)-A is less stable by 0.13 eV per CH than 2D graphane-A; graphene itself is also more stable per carbon atom than all fullerenes and all nanotubes.[13] If one looks at the CC distances (Table 1) and CCC angles (not shown here) one sees signs of

substantial strain (long and short bonds compared to the 1.54 Å of a normal CC bond, angles distorted from tetrahedral). The strain caused in some of these structures by curving into a tube form is likely to be substantial.

More than 0.6 eV per CH separate the most and least stable graphane nanotubes. The reason for this spread, and a rough understanding of the detailed ordering of these structures in energy may be found in the H···H contacts. Table 1 lists the computed bond distances in pure carbon systems (graphene, single-wall nanotubes (10,0) and (10,10)), 2D graphane sheets, and 1D graphane nanotubes. Note first of all the expected CC distances −1.42 Å in graphene and nanotubes, and at around 1.54 Å on the short side of the range for this distance in graphane and GN structures. A molecular model for the C−C distance might be 2,3-dimethylbutane, $(CH_3)_2CH-CH(CH_3)_2$. The central bond in this molecule is calculated to be 1.55 Å in either eclipsed or staggered orientations (see the Supporting Information). The longer CC distances in the GNs, those >1.60 Å, are signs of great strain in these structures.

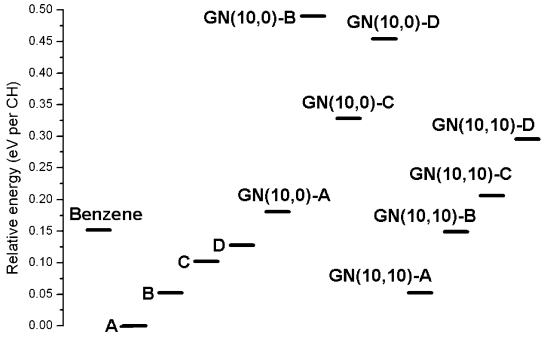


**Figure 3. The relative energy (in eV per CH; the zero of energy is the single-sheet graphane-A, 0 K) of benzene, four single-sheet graphanes, four graphane nanotubes GN (10,0) and four graphane nanotubes GN (10,10).**

One can use the calculated CC distances to get an idea of just how much strain might be involved. This may be done with the same molecular model, 2,3-dimethylbutane, by calculating a potential energy curve for stretching (or contracting) the central CC bond in the molecule.[14] This is done in the Supporting Information; to elongate the CC bond in the molecular model to 1.72 Å (the maximum such CC distance in GN (10−0)-B in Table 1) costs 6 kcal/mol.

Note first of all that the larger diameter (10,10) GNs are ordered in energy just as the graphane sheets they are based on, but somewhat more differentiated in energy. In rationalizing the computed stability of graphane three-dimensional crystals under pressure we found useful an argument based on the shorter H···H distances in any structure.[6] Let us see where this kind of reasoning will take us for the GNs. We need a "normal" H···H contact, an unstrained van der Waals minimum, to compare against. This might be provided by planar graphane-A (2.54 Å) and B (2.25 Å) in their calculated $P$ = 1 atm crystal structures.

One way to think about the sterically encumbered hydrogens in the interior of the graphane nanotubes is to consider them being under "intramolecular pressure". We could, for instance, go back to our calculations of unstrained graphane sheets under pressure, and look at what pressure the *inter*molecular H···H contacts between two graphane sheets would come to be as short as the *intra*molecular H···H contacts in GN(10,10)-A (see Supporting Information for calculation). That condition is reached at about 250 GPa pressure on the graphane nanosheets.

**TABLE 1. Calculated Relative Energy, $E_{rel}$ (eV per C or CH), C−C Distance, the Shortest H−H (Å), Diameter $D$ (the Longest Distance among the Inner H atoms, Å) and the Calculated HSE and PBE Band Gaps for Graphene, SWNT (10,0), SWNT(10,10), Four Single-Sheet Graphanes, Four Graphane SWNTs (10,0), and Four Graphane SWNTs (10,10)**

| | | $E_{rel}$ (eV) | C−C (Å) | shortest H−H (Å) | $D$ (Å) | HSE Gap (eV) | PBE Gap (eV) |
|---|---|---|---|---|---|---|---|
| pure C phase | graphene | (0.00) | 1.43 | | ∞ | 0.0 | 0.0 |
| | SWNT (10, 0) | (0.13) | 1.42, 1.43 | | 7.9 | 1.0 | 0.8 |
| | SWNT(10, 10) | (0.04) | 1.43 | | 13.6 | 0.0 | 0.0 |
| graphane | A | [0.00] | 1.54 | 2.54 | ∞ | 4.0 | 3.5 |
| | B | [0.05] | 1.54 | 2.25 | ∞ | 4.0 | 3.5 |
| | C | [0.10] | 1.54, 1.57 | 2.10 | ∞ | 4.0 | 3.5 |
| | D | [0.13] | 1.54, 1.57 | 2.12 | ∞ | 4.0 | 3.5 |
| GN(10, 0) | GN (10, 0)-A | [0.18] | 1.56 | 1.76 | 5.7 | 4.0 | 3.5 |
| | GN (10, 0)-B | [0.49] | 1.50, 1.51, 1.72 | 1.80 | 5.8 | 3.5 | 3.0 |
| | GN (10, 0)-C | [0.33] | 1.56, 1.58 | 1.72 | 5.6 | 3.5 | 3.0 |
| | GN (10, 0)-D | [0.46] | 1.55, 1.57, 1.61 | 1.37 | 4.1 | 2.0 | 1.5 |
| GN(10, 10) | GN (10, 10)-A | [0.05] | 1.54 | 2.20 | 11.5 | 4.0 | 3.5 |
| | GN (10, 10)-B | [0.15] | 1.55, 1.56 | 1.84 | 9.7 | 3.5 | 3.0 |
| | GN (10, 10)-C | [0.21] | 1.54, 1.57, 1.62 | 1.62 | 11.3 | 3.8 | 3.3 |
| | GN (10, 10)-D | [0.30] | 1.53, 1.57, 1.67 | 1.58 | 11.3 | 3.0 | 2.8 |

The H···H contacts in the interior of the (10,10) GNs get progressively shorter, and definitely are in the region where their energy penalizes the GN(10,10)-B, C, D structures (see Table 1). Also the more stable the structure in this series, the less are the CC bonds elongated −1.54 Å in GN(10,10)-A, up to 1.67 Å in GN(10,10)-D.

Their elongated C−C distances and too short H···H contacts clearly show that the (10,0)-nanotubes are in trouble, and the energies reflect that. There is a lot of strain in these structures, arising from through-space H···H interaction in the repulsive region of the van der Waals potential, as well as eclipsing *versus* staggering in the C network, and other tensions, introduced by the conflict of tube formation and the important desire of C for an approximately tetrahedral environment. Just as for the pure C nanotubes, the diameter of the tube matters, with strain exacerbated in small diameter tubes. The nanotube diameter *D* (the longest separation, between the inner hydrogen carbons of the nanotube), at 4.1−5.8 Å for the (10,0) GNs, is clearly small.

We proceeded to a further study of GN properties, focusing on the most stable GN(10,10)-A.

**Electronic Properties of GN (10,10)-A.** Normal DFT calculations, such as we use, systematically underestimate band gaps.[15] We therefore proceeded to hybrid functional calculations (HSE) which generally produce a more realistic band gap;[16−18] the calculated HSE band gaps (see Table 1 and the density of states shown in the Supporting Information) for the graphane-A and 1D GN(10,10)-A are around 4.0 eV. We will revisit the HSE bang gap later. It is clear that these GN structures will be wide-band insulators. For comparison, the corresponding PBE band gaps are listed in Table 1; they are lower than the HSE values.

**Annealing Analysis of Graphane-A and GN(10,10)-A.** DFT computations apply to the ground state situation. What might be the effect of temperature on graphane-A and GN(10,10)-A? To analyze this, we run an annealing simulation, heating up to 2000 K, and cooling down to 300 K. The calculated temperature and energy profile are plotted in Figure 4 (left) for graphane-A and (right) for GN(10,10)-A. From Figure 4, one can see that for both graphane-A and GN(10,10)-A, the temperature varies almost linearly, with a less fluctuating energy profile, of course moving to lower energy at lower temperatures. In general, the large energy fluctuations indicate that there are rather big structural changes at each simulation step. After annealing, the final structure of graphane-A and GN(10,10)-A still looks very much like the corresponding initial structure, indicative of stability.

To get some further insight into the departures from regularity on heating, we compute a root-mean-square deviation (rmsd), rmsd = $((\sum_{i=1}^{n}(r_i - r_0)^2)/n)^{1/2}$, where, $r_0$ and $r_i$ are the bond distances in initial and final structure, respectively; *n* is the number of bonds. We calculate the rmsd of the C−C and C−H bonds in both graphane-A and GN (10,10)-A. The rmsd values for the C−C and C−H in graphane are 0.027 and 0.024, respectively, while the values for C−C and C−H are 0.021 and 0.019 in GN (10,10)-A, respectively, indicating small changes on both structures.

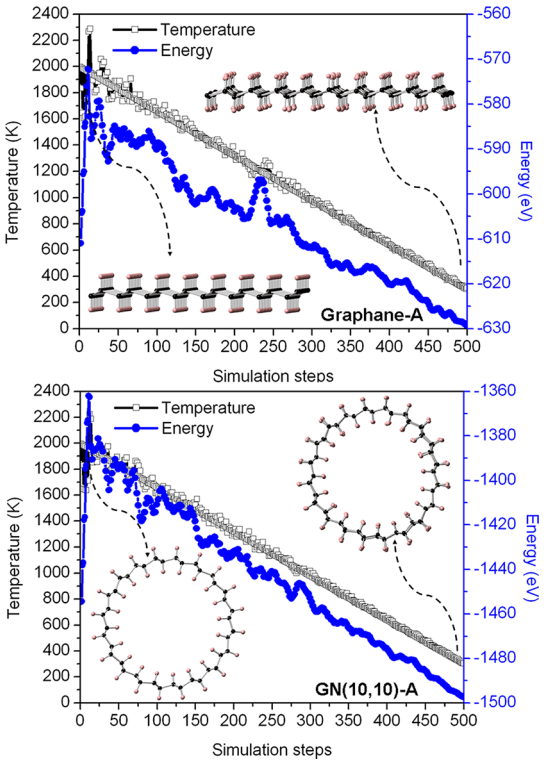


**Figure 4. (Top) Calculated temperature and energy profile for annealing graphane-A. The initial and final structure is inserted. (Bottom) Calculated temperature and energy profile for annealing GN(10,10)-A. The initial and final structure is inserted. The energy values are internal energy.**

**A Possible Reaction Relating Graphane and GN(10,10)-A.** In 2009, Elias *et al.*[5] devised a way to make graphane by passing hydrogen gas through an electrical discharge at fairly low temperatures (around room temperature). This creates hydrogen atoms, which then drift toward a sample of graphene and bond with its carbon atoms.

One might then imagine that one way (there may be others) of synthesizing GNs might be by reaction of all-C nanotubes and $H_2$. The reaction can be written as

$$C_x(s) + \frac{x}{2} H_2(g) \rightarrow xCH(s)$$

To determine the reaction energy of the process, the relative energy and free energy of the reaction can be obtained from eq a which can be further approximated by expression b.

$$\Delta G = x[\mu(CH(s))] - \mu(C_x(s)) - \frac{x}{2}[\mu(H_2)] \quad \textbf{(a)}$$

$$\Delta G = \Delta E_0 - \frac{x}{2}\Delta\mu(T, P_{H_2}) \quad \textbf{(b)}$$

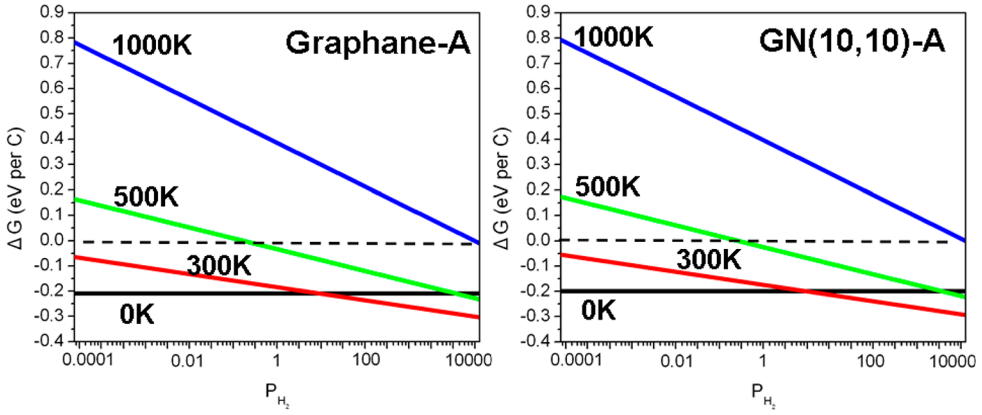


**Figure 5. Free energies (Δ*G*) per carbon for graphane-A and GN(10,10)-A as a function of the $P_{H_2}$ at various temperature.**

Here, $\Delta E_0$ is the difference between the electronic energies of the products and reactants at 0 K. $\Delta\mu(T, P_{H_2})$ is the difference of the chemical potentials of the $H_2$ gas phase in the reaction:

$$\Delta\mu(T, P_{H_2}) = \Delta\mu^o(T) + RT \ln(P_{H_2}) \qquad \textbf{(c)}$$

$\Delta\mu^o(T)$ is the corrected free energy change computed from calculations of $H_2$ that include zero point energies. $P_{H_2}$ is the partial pressure of $H_2$ gas. Combining eqs c and b, one gets

$$\Delta G = \Delta E_0 - \frac{x}{2}[\Delta\mu^o(T) + RT \ln(P_{H_2})] \qquad \textbf{(d)}$$

In our thermodynamic calculations, we consider temperatures of 300, 500, and 1000 K, respectively. The $\Delta\mu^o$(T) in eV for $H_2$ are then calculated to be −0.052 at 300 K, −0.35 at 500 K and −1.19 eV at 1000 K. Note that the free energy calculated here includes both enthalpy and entropy contributions.

Figure 5 shows the calculated variation of the free energy change for formation of graphane-A (left) and GN(10,10)-A (right) from graphene or the all-C nanotube, respectively, as a function of partial pressure of $H_2$ gas (between 0.0001 and 10000 Pa) at various temperatures (from 300 to 1000 K). One can see that the synthesis of graphane-A and GN(10,10)-A at 0 and 300 K is thermodynamically favorable, over the whole range of partial pressure of $H_2$ considered. At high temperatures (1000 K) the process becomes unfavorable. Interestingly, the equilibrium of the reaction for graphane-A and GN(10,10)-A can be shifted by varying the partial pressure of $H_2$ gas, as one can see from the curves at 500 K, which cross the dotted line (of zero Δ*G*) when $P_{H_2}$ is around 1 Pa. We conclude that graphane-A and GN(10,10)-A can be made from graphene and nanotubes, respectively, at low temperature and high partial pressure of $H_2$ gas. High temperatures may not only damage the crystal structure of graphene or nanotubes, but also shift the equilibrium of the reactions.

**The Effect of Size on Armchair GN Structures.** Given the computed stability of armchair-type GN (10,10)-A, we build several armchair-type graphane nanotubes with smaller diameters, including GN(7,7)-A, GN(5,5)-A, and GN(3,3)-A. Table 2 lists the calculated relative energies, bond distances, and diameters for these armchair-type GN structures, as well the computed (HSE functional) band gap. As expected, the smaller the diameter is , the closer to each other are the inner Hs, and the less stable (relative to the graphane sheet) is the GN. In addition, zigzag-type graphane nanotubes of different sizes, GN(15,0)-A, GN(10,0)-A, and GN(7,0)-A have been computed (see Table 2). GN(15,0) is the most stable configuration among these. However, it is still 0.02 eV per CH higher in energy than the armchair-type GN(10,10)-A. The zigzag type graphane nanotubes are also computed to be insulators.

**TABLE 2. Calculated Relative Energy, $E_{rel}$ (eV per C or CH), C−C, and the Shortest H−H Distance (Å), Tube Diameter (*D*, Å) for Graphene, SWNT (10,0), SWNT(10,10), Four Single-Sheet Graphanes, Four Graphane SWNTs (10,0) and Four Graphane SWNTs (10,10), and Calculated HSE and PBE Band Gaps**

| | | $E_{rel}$ | | shortest | | HSE | PBE |
|---|---|---|---|---|---|---|---|
| | | eV | C−C Å | H−H Å | *D* Å | gap eV | gap eV |
| graphane | A | [0.00] | 1.54 | 2.54 | ∞ | 4.0 | 3.5 |
| armchair GN | GN (10,10)-A | [0.05] | 1.54 | 2.20 | 11.50 | 4.0 | 3.5 |
| | GN (7.7)-A | [0.10] | 1.55 | 2.06 | 7.25 | 4.1 | 3.4 |
| | GN (5,5)-A | [0.22] | 1.57 | 1.90 | 4.70 | 4.3 | 3.5 |
| | GN (3,3)-A | [0.70] | 1.64 | 1.65 | 2.10 | 5.3 | 4.3 |
| zigzag GN | GN (15,0)-A | [0.07] | 1.55 | 2.00 | 9.6 | 3.8 | 3.1 |
| | GN (10,0)-A | [0.18] | 1.56 | 1.76 | 5.7 | 4.0 | 3.5 |
| | GN (7,0)-A | [0.42] | 1.59 | 1.51 | 3.4 | 4.7 | 4.0 |

Figure 6 shows the computed HSE band gaps for GN(3,3)-A, GN(5,5)-A, GN(7,7)-A, GN(10,10)-A, and graphane-A as a function of the corresponding shortest distance H···H separation. Usually, structures containing CC and CH bonds show a band gap decrease with strain; these systems behave in an opposite way. The computed band gap trend for the armchair GNs is also found for the zigzag type, see Table 2.

Figure 7 shows the corresponding free energy ($\Delta G$) for GN(3,3)-A, GN(5,5)-A, GN(7,7)-A, and GN(10,10)-A as a function of the $P_{H_2}$ at 300 and 500 K, respectively. Note that the free energy of the graphane nanotubes (GN(N,N)) is related to the corresponding carbon nanotubes (SWNT(N,N)) and $H_2$. In experiment, single-walled, all-carbon nanotubes (N,N) with $N = 5$ (approximate diameter, $D$, 6.8 Å), 7 ($D \approx 9.5$ Å) and 10 ($D \approx 13.6$ Å) have been synthesized,[19] while the SWNT(3,3) with a diameter at ~4.0 Å also was found inside of double-walled carbon nanotubes.[20] The thinnest freestanding single-walled carbon nanotube known is about 4.3 Å in diameter.

The free energies (Figure 7) indicate that GN(5,5)-A, GN(7,7)-A, and GN(10,10)-A could be stable over the entire range of $P_{H_2}$ at 300 K. At 500 K, the reactions become favorable only under high partial pressure of $H_2$ gas. It is not surprising that GN(3,3)-A, the narrowest tube, should be the hardest to synthesize among these graphane nanotubes. We emphasize that the hydrogenation reaction is only one way to make these graphane nanotubes, and we do not exclude other methods.

**Partially Hydrogenated Nanotubes.** Partial hydrogenation of all C nanotubes is not only a realistic outcome of most experimental hydrogenation protocols, but also a way to engineer band gaps. Studies on partially hydrogenated nanotubes[8,21−24] (primarily focusing on the hydrogenation on the outside), graphene,[25−30] and fullerenes (some of them are fully hydrogenated)[9−12] have been published. There is much to be learned from this work—for instance it is clear from angle strain considerations that complete hydrogenation on the outside of a fullerene is totally unlikely, and that some inside and some outside hydrogenation is a good compromise. The hydrogenated structures presented by us are, however, different, in that they begin with a nanotube and then, using a graphane nanotube as a model, hydrogenate on the inside and the outside a variable, translationally periodic part of the nanotube. We begin with all-C SWNT (10,10), and proceed to hydrogenate it in stages, using graphene itself as a calibration.

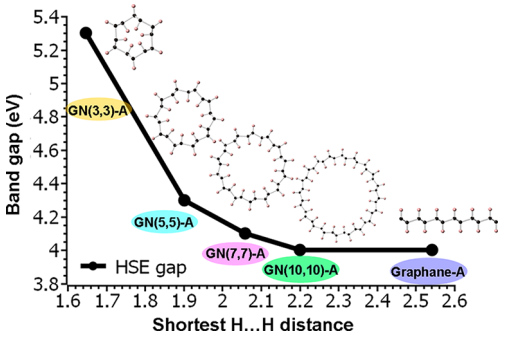


**Figure 6. Computed HSE band gaps for GN(3,3)-A, GN(5,5)-A, GN(7,7)-A, GN(10,10)-A and graphane-A as a function of the corresponding shortest inner H···H separation in the structures.**

We examined structures for 6 carbons (19%), 16 carbons (50%), and 26 carbons (80%) hydrogenated of a graphene supercell with 32 carbons. The corresponding optimized partially hydrogenated graphene structures are shown in Figure 8 (left). Figure 8 (right) shows the 20% (8 carbons), 50% (20 carbons), and 80% (32 carbons) hydrogenated SWNT(10,10) with 40 carbons. Graphane-A-type termination is assumed.

We might expect, and indeed we obtain (Figure 9), some deformation of the nanotube cylinder for the partially hydrogenated SWNT(10,10). Figure 9 shows the corresponding free energy ($\Delta G$, relative to graphene + $H_2$ and SWNT(10,10) + $H_2$) for partially hydrogenated graphene (at left) and partially hydrogenated SWNT(10,10) (at right) as a function of the $P_{H_2}$ at 300 K, respectively. The more hydrogenation there is (whether of graphene, or the all-C nanotube), the more stable is the resulting structure. From a comparison of the free energies of hydrogenation of graphene and nanotube, it appears that at 300 K hydrogenation of the nanotube is favored.

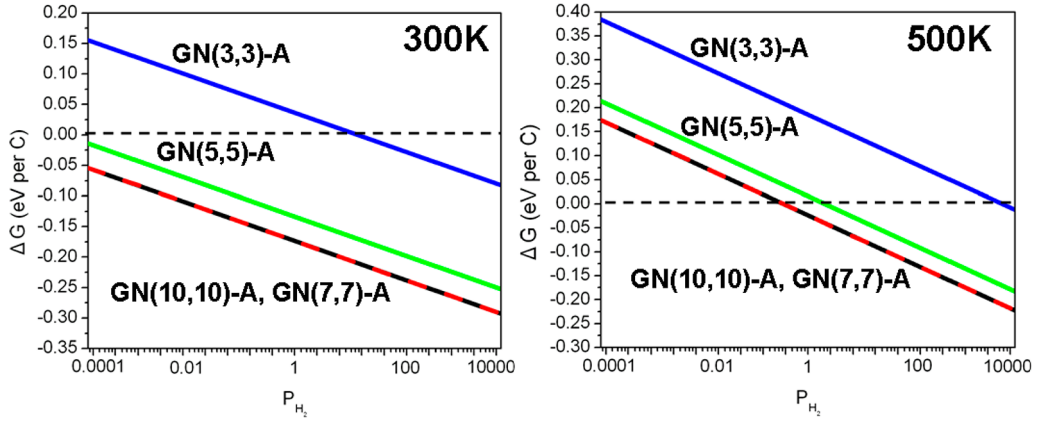


**Figure 7. Free reaction energies ($\Delta G$) per carbon for armchair graphane nanotubes as a function of the $P_{H_2}$ at 300 and 500 K, respectively.**

The interest in these partially hydrogenated structures lies in the opportunity they provide of engineering band gaps. Table 3 shows the calculated HSE and PBE band gap for graphene, SWNT(10,10), and their corresponding hydrogenated species. Interestingly, the 19% and 50% hydrogenated graphenes are in our calculations metallic, while a large band gap is found in the 80% hydrogenated graphene (see Supporting Information). The calculated DOS for SWNT-(10,10) with 20% and 50% hydrogenation shows they are still metallic, while the structure with 80% hydrogenated SWNT(10,10) is computed to be a semiconductor with a band gap of 1.0 eV. The results show that the band gap of graphene or SWNT can be significantly tuned *via* hydrogenation, as also suggested by some research groups working on graphene and its partial hydrogenation.[28,31]

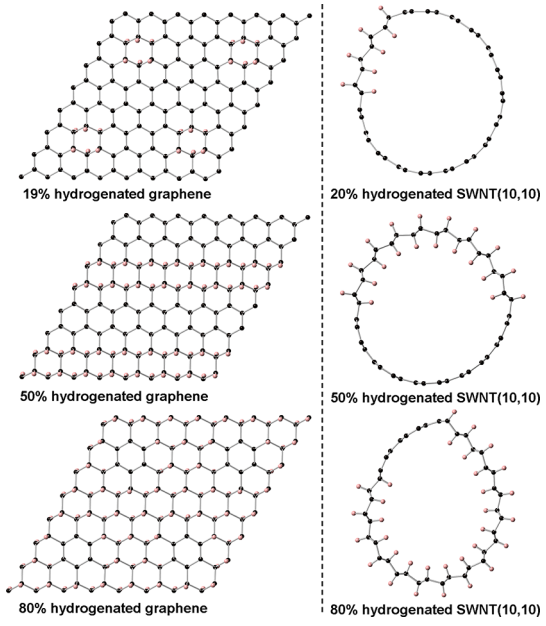


**Figure 8. (Left) Partially hydrogenated (19%, 50%, and 80%) graphene configurations. (Right) partially hydrogenated (20%, 50%, and 80%) SWNT(10,10) configurations. More views and configurations considered can be found in the Supporting Information.**

## CONCLUSIONS

In a previous study, we investigated systematically some two-dimensional (2D) single-sheet graphanes and 3D crystals of such graphanes under high pressure (up to 300 GPa). In this work, one-dimensional (1D) graphane nanotubes (GN) were designed from the four most stable 2D single-sheet graphanes, and were systematically examined. Two types of nanotubes, armchair (10,10) and zigzag (10,0) type GNs, were chosen for initial consideration. Each graphane isomer (A, B, C, D) then leads to two nanotubes. GN(10,10)-A is calculated to be the most stable configuration among these GN structures; it is lower in energy per CH than the benzene molecule, but unstable thermodynamically (yet no doubt kinetically persistent) relative to graphane-A, due to strain. If we go by the HH separations in the interior of the nanotube and compare to compressed 3D crystals of graphanes, the interior pressure in the GNs approaches 250 GPa. The calculated band gaps show all of GNs are insulators; the

**TABLE 3. Calculated HSE and PBE Band Gaps for Graphene, Graphane-A, SWNT(10,10), GN(10,10)-A, Three Partially Hydrogenated Graphenes and Three Partially Hydrogenated SWNTs(10,10)**

| | | HSE Gap (eV) | PBE Gap (eV) |
|---|---|---|---|
| 2D system | graphene | 0.0 | 0.0 |
| | 19% hydrogenated graphene | 0.0 | 0.0 |
| | 50% hydrogenated graphene | 0.0 | 0.0 |
| | 80% hydrogenated graphene | 4.5 | 3.8 |
| | 100% hydrogenated graphene | 4.0 | 3.5 |
| 1D system | SWNT (10, 10) | 0.0 | 0.0 |
| | 20% hydrogenated SWNT(10,10) | 0.0 | 0.0 |
| | 50% hydrogenated SWNT(10,10) | 0.0 | 0.0 |
| | 80% hydrogenated SWNT(10,10) | 1.0 | 1.0 |
| | 100% hydrogenated SWNT(10,10) | 4.0 | 3.5 |

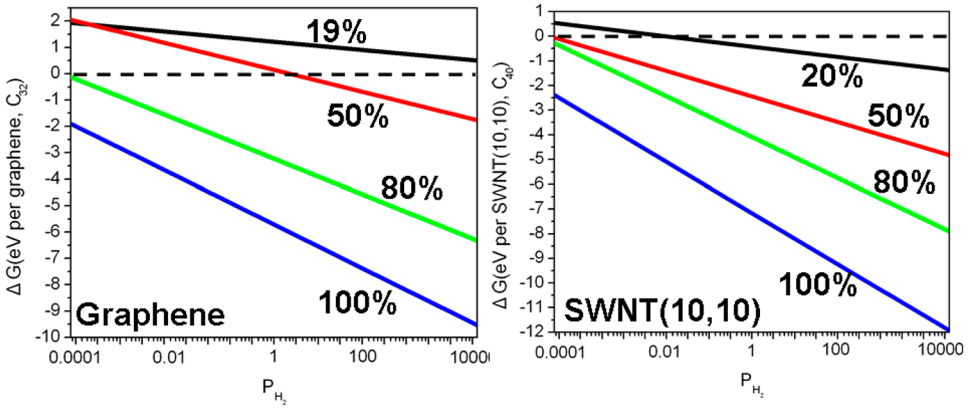


**Figure 9. (Left) Free reaction energies ($\Delta G$) per graphene for partially hydrogenated graphene configurations as a function of the $P_{H_2}$ at 300 K; (Right) Free reaction energies ($\Delta G$) for partially hydrogenated SWNT(10,10) configurations as a function of the $P_{H_2}$ at 300 K.**

band gap depends on both the size (the diameter of GNs) and hydrogenation of the nanotube. The results on the partially hydrogenated graphene and SWNT indicate that the greater the degree of hydrogenation, the more stable the resulting structure.

On performing an annealing simulation (by *ab initio* molecular dynamics), the final structures of graphane-A and GN(10,10)-A still appear very much like the corresponding initial structure, indicative of stability. The relative stability of the nanotube can be measured by the enthalpy of the reaction ($C_x + {}^{x}/_{2}H_2 \rightarrow xCH$) for forming the GN, as a function of temperature and pressure. We conclude that graphane-A and GN(10,10)-A might therefore be synthesized at low temperature and high partial pressure of $H_2$ gas from graphene and nanotubes, respectively.

**Computational Methods.** The calculations are based on the plane wave/pseudopotential approach using the computer program VASP (Vienna *Ab-Initio* Simulation Package 5.2.11),[32] employing the PBE exchange-correlation functional[33,34] and the projector-augmented wave (PAW)[35,36] method. The energy cutoff for the plane-wave basis was set to 600 eV. The Brillouin zone was sampled by $1 \times 1 \times 15$ Monkhorst-Pack meshes for these 1D graphane nanotubes. Since VASP computes only three-dimensional structures, to model a 1D structure we used a 3-D unit cell with >30 Å along a and *b* axis. The relaxation of the electronic degrees of freedom was stopped if the total (free) energy change and the band structure energy change between two steps was both smaller than $1 \times 10^{-6}$. A conjugate-gradient algorithm was used to relax the ions into their instantaneous ground state. An annealing simulation using the *ab initio* molecular dynamic method (Born–Oppenheimer *ab initio* molecular dynamics (MD) implemented in VASP code) is performed to generate random configurations and to investigate the stability of the derived optimized structures. For the annealing process, the initial temperature of the system is increased to 2000 K, and a final temperature of 300 K is requested. The total number of simulation steps is 500, each 1 fs long since the CH stretching motion has a period of 11–12 fs. In our work, for the hybrid functional calculations (HSE), the $\omega$ is defined as 0.207 $Å^{-1}$ as originally suggested by Heyd *et al.*[16]

*Conflict of Interest:* The authors declare no competing financial interest.

*Acknowledgment.* We thank the reviewers of this paper for bringing some work we missed to our attention. Our work at Cornell was supported by the National Science Foundation through Grants CHE-0613306 and CHE-0910623 and by DMR-0907425; it was also supported by the EFree program at Carnegie Institution of Washington for the Department of Energy. This research also received support from the National Science Foundation through TeraGrid resources provided by NCSA. X.-D. Wen gratefully acknowledges a Seaborg Institute Fellowship (the LDRD program at LANL). The Los Alamos National Laboratory is operated by Los Alamos National Security, LLC, for the National Nuclear Security Administration of the U.S. Department of Energy under Contract DE-AC5206NA25396.

*Supporting Information Available:* (1) More views on graphane nanotubes and the calculated density of states for them; (2) optical properties of Graphane-A and GN(10,10)-A; (3) molecular model for the C–C distance in 2,3-dimethylbutane; (4) *inter*molecular and *intra*molecular H···H contacts in Graphane-I, II, III, IV and V as a function of pressure; (5) partially hydrogenated SWNT(10,10) and graphene structures, as well the calculated density of states. This material is available free of charge *via* the Internet at http://pubs.acs.org.

## REFERENCES AND NOTES

1. Kara, A.; Enriquez, H.; Seitsonen, A. P.; Lew Yan Voon, L. C.; Vizzini, S.; Aufray, B.; Oughaddou, H. A Review on Silicene—New Candidate for Electronics. *Surf. Sci. Rep.* **2012**, *67*, 1–18.
2. Bushan, B., Ed. *Springer Handbook of Nanotechnology*, 3rd ed.; Springer, Heidelberg, 2010.
3. Sluiter, M. H. F.; Kawazoe, Y. Cluster Expansion Method for Adsorption: Application to Hydrogen Chemisorption on Graphene. *Phys. Rev. B* **2003**, *68*, 085410.
4. Sofo, J. O.; Chaudhari, A.; Barber, G. D. Graphane: A Two-Dimensional Hydrocarbon. *Phys. Rev. B* **2007**, *75*, 153401.
5. Elias, D. C.; Nair, R. R.; Mohiuddin, T. M. G.; Morozov, S. V.; Blake, P.; Halsall, M. P.; Ferrari, A. C.; Boukhvalov, D. W.; Katsnelson, M. I.; Geim, A. K.; Novoselov, K. S. Control of Graphene's Properties by Reversible Hydrogenation: Evidence for Graphane. *Science* **2009**, *323*, 610–613.
6. Wen, X.-D.; Hand, L.; Labet, V.; Yang, T.; Hoffmann, R.; Ashcroft, N. W.; Artem, R. O.; Andriy, O. L. Graphane Sheets and Crystals Under Pressure. *Proc. Natl. Acad. Sci. U.S.A.* **2011**, *108*, 6833–6837.
7. Hoffmann, R. One Shocked Chemist. *Am. Sci.* **2011**, *99*, 116–119.
8. Lu, X.; Chen, Z. Curved Pi-Conjugation, Aromaticity, and the Related Chemistry of Small Fullerenes (<$C_{60}$) and Single-Walled Carbon Nanotubes. *Chem. Rev.* **2005**, *105*, 3643–3696.
9. Saunders, M. Buckminsterfullerane: The Inside Story. *Science* **1991**, *253*, 330–331.
10. Jia, J.; Wu, H.-S.; Xu, X.-H.; Zhang, X.-M.; Jiao, H. Fused Five-Membered Rings Determine the Stability of $C_{60}F_{60}$. *J. Am. Chem. Soc.* **2008**, *130*, 3985–3988.
11. Jia, J.; Wu, H.-S.; Xu, X.-H.; Zhang, X.-M.; Jiao, H. Tube and Cage $C_{60}H_{60}$: A Comparison with $C_{60}F_{60}$. *Org. Lett.* **2008**, *10*, 2573–2576.
12. Zdetsis, A. D. Structural, Cohesive, Electronic, and Aromatic Properties of Selected Fully and Partially Hydrogenated Carbon Fullerenes. *J. Phys. Chem. C* **2011**, *115*, 14507–14516.
13. Wen, X.-D.; Cahill, T. J.; Hoffmann, R. Exploring Group 14 Structures: 1D to 2D to 3D. *Chem.—Eur. J.* **2010**, *16*, 6555–6566.
14. Huntley, D. R.; Markopoulos, G.; Donovan, P. M.; Scott, L. T.; Hoffmann, R. Squeezing C–C Bonds. *Angew. Chem., Int. Ed.* **2005**, *44*, 7549–7553.
15. Hafner, J. *Ab-Initio* Simulations of Materials Using VASP: Density-Functional Theory and Beyond. *J. Comput. Chem.* **2008**, *29*, 2044–2078.
16. Heyd, J.; Scuseria, G. E.; Ernzerhof, M. Hybrid Functionals Based on A Screened Coulomb Potential. *J. Chem. Phys.* **2003**, *118*, 8207.
17. Heyd, J.; Scuseria, G. E.; Ernzerhof, M. Erratum: "Hybrid Functionals Based on a Screened Coulomb Potential. *J. Chem. Phys.* **2006**, *124*, 219906.
18. Heyd, J.; Peralta, J. E.; Scuseria, G. E.; Martin, R. L. Energy Band Gaps and Lattice Parameters Evaluated with the Heyd–Scuseria–Ernzerhof Screened Hybrid Functional. *J. Chem. Phys.* **2005**, *123*, 174101.
19. Reich, S.; Thomsen, C.; Maultzsch, J. *Carbon Nanotubes: Basic Concepts and Physical Properties*, Wiley-VCH: Germany, 2007.
20. Lunhui, G.; Kazu, S.; Sumio, I. Smallest Carbon Nanotube Assigned with Atomic Resolution Accuracy. *Nano Lett.* **2008**, *8*, 459–462.

21. Maiti, A. Energetic Stability of Hydrogen-Chemisorbed Carbon Nanotube Structures. *Chem. Phys. Lett.* **2011**, *508*, 107–110.
22. Lee, K. W.; Lee, C. E. Half-Metallic Carbon Nanotubes. *Adv. Mater.* **2012**, *24*, 2019–2023.
23. Chen, Z.; Thiel, W.; Hirsch, A. Reactivity of the Convex and Concave Surfaces of Single-Walled Carbon Nanotubes (SWCNTs) towards Addition Reactions: Dependence on the Carbon-Atom Pyramidalization. *ChemPhysChem* **2003**, *1*, 93–97.
24. Zhou, Z.; Zhao, J.; Chen, Z.; Gao, X.; Yan, T.; Wen, B.; Schleyer, P.; von, R. Comparative Study of Hydrogen Adsorption on Carbon and BN Nanotubes. *J. Phys. Chem. B* **2006**, *110*, 13363–13369.
25. Li, Y.; Chen, Z. Patterned Partially Hydrogenated Graphene ($C_4H$) and Its One-Dimensional Analogues: A Computational Study. *J. Phys. Chem. C* **2012**, *116*, 4526–4534.
26. Sarkar, S.; Bekyarov, E.; Haddon, R. C. Chemistry at the Dirac Point: Diels-Alder Reactivity of Graphene. *Acc. Chem. Res.* **2012**, *45*, 673–682.
27. Li, Y.; Zhou, Z.; Shen, P.; Chen, Z. Structural and Electronic Properties of Graphane Nanoribbons. *J. Phys. Chem. C* **2009**, *113*, 15043–15045.
28. Chandrachud, P.; Pujari, B. S.; Haldar, S.; Sanyal, B.; Kanhere, D. G. A Systematic Study of Electronic Structure from Graphene to Graphane. *J. Phys.: Condens. Matter.* **2010**, *22*, 465502 and references within it.
29. Haldar, S.; Kandere, D. G.; Sanyal, B. Magnetic Impurities in Graphane with Dehydrogenated Channels. *Phys. Rev. B* **2012**, *85*, 155426.
30. Kim, H.-J.; Oh, S.; Zeng, C.; Cho, J.-H. Peierls Instability and Spin Orderings of Ultranarrow Graphene Nanoribbons in Graphane. *J. Phys. Chem. C,* **2012**, *116*, 13795–13799.
31. Duplock, E. J.; Scheffler, M.; Lindan, P. J. Hallmark of Perfect Graphene. *Phys. Rev. Lett.* **2004**, *92*, 225502.
32. Kresse, G.; Hafner, J. *Ab Initio* Molecular Dynamics for Liquid Metals. *Phys. Rev. B* **1993**, *47*, 558–561.
33. Perdew, J. P.; Burke, K.; Ernzerhof, M. Generalized Gradient Approximation Made Simple. *Phys. Rev. Lett.* **1996**, *78*, 3865–3868.
34. Perdew, J. P.; Burke, K.; Ernzerhof, M. Errata: Generalized Gradient Approximation Made Simple. *Phys. Rev. Lett.* **1997**, *78*, 1396–1396.
35. Bloechl, P. E. Projector Augmented-Wave Method. *Phys. Rev. B* **1994**, *50*, 17953–17979.
36. Kresse, G.; Joubert, D. From Ultrasoft Pseudopotentials to the Projector Augmented-Wave Method. *Phys. Rev. B* **1999**, *59*, 1758–1775.